JOURNAL OF BACTERIOLOGY, Dec. 2000, p. 6605–6613 Vol. 182, No. 23
0021-9193/00/$04.00+0

Structural and Kinetic Characterization of an Archaeal β-Class Carbonic Anhydrase

KERRY S. SMITH,[1] NATHANIEL J. COSPER,[2] CHRISTINA STALHANDSKE,[2]† ROBERT A. SCOTT,[2] AND JAMES G. FERRY[1]*

Department of Biochemistry and Molecular Biology, The Pennsylvania State University, University Park, Pennsylvania 16802,[1] and Center for Metalloenzyme Studies, University of Georgia, Athens, Georgia 30602-2556[2]

Received 17 May 2000/Accepted 11 September 2000

The β-class carbonic anhydrase from the archaeon *Methanobacterium thermoautotrophicum* (Cab) was structurally and kinetically characterized. Analytical ultracentrifugation experiments show that Cab is a tetramer. Circular dichroism studies of Cab and the *Spinacia oleracea* (spinach) β-class carbonic anhydrase indicate that the secondary structure of the β-class enzymes is predominantly α-helical, unlike that of the α- or γ-class enzymes. Extended X-ray absorption fine structure results indicate the active zinc site of Cab is coordinated by two sulfur and two O/N ligands, with the possibility that one of the O/N ligands is derived from histidine and the other from water. Both the steady-state parameters k_{cat} and k_{cat}/K_m for CO_2 hydration are pH dependent. The steady-state parameter k_{cat} is buffer-dependent in a saturable manner at both pH 8.5 and 6.5, and the analysis suggested a ping-pong mechanism in which buffer is the second substrate. At saturating buffer conditions and pH 8.5, k_{cat} is 2.1-fold higher in H_2O than in D_2O, consistent with an intramolecular proton transfer step being rate contributing. The steady-state parameter k_{cat}/K_m is not dependent on buffer, and no solvent hydrogen isotope effect was observed. The results suggest a zinc hydroxide mechanism for Cab. The overall results indicate that prokaryotic β-class carbonic anhydrases have fundamental characteristics similar to the eukaryotic β-class enzymes and firmly establish that the α-, β-, and γ-classes are convergently evolved enzymes that, although structurally distinct, are functionally equivalent.

The thermophilic archaeon *Methanobacterium thermoautotrophicum* obtains energy for growth by the reduction of CO_2 to CH_4 and is also an obligate chemolithoautotroph; thus, this organism has a high demand for CO_2. Carbonic anhydrase, a zinc-containing enzyme catalyzing the reversible hydration of carbon dioxide (equation 1)

$$CO_2 + H_2O \rightleftharpoons HCO_3^- + H^+ \quad (1)$$

is expected to play an important role in the growth of *M. thermoautotrophicum* and may have several functions, including transporting HCO_3^- into the cell and providing CO_2 or HCO_3^- to enzymes that utilize these substrates.

Based on sequence comparisons, carbonic anhydrases belong to three genetically distinct classes (α, β, and γ) which appear to have independent origins (24). The most extensively studied enzymes are those from the α-class, which is composed primarily of mammalian carbonic anhydrases, but also includes enzymes from the green alga *Chlamydomonas reinhardtii* (19, 20) and the prokaryote *Neisseria gonorrhoeae* (13). The β-class enzymes are abundant in C_3 and C_4 monocotyledenous and dicotyledenous plants and green unicellular algae (24, 43), where they are essential for photosynthetic CO_2 fixation (6). The most recently identified class of carbonic anhydrase, the γ-class (24), is represented by the prototype Cam from the archaeon *Methanosarcina thermophila* (2). Even though sequences encoding putative γ-class carbonic anhydrases have been found in prokaryotes from both the *Bacteria* and *Archaea* domains (2, 52), Cam is the only γ-class enzyme that has been biochemically characterized (2, 3, 58).

Crystal structures for five α-class mammalian isozymes (CA I to V) (10, 16, 17, 23, 33, 38, 54) and the α-class enzyme from *N. gonorrhoeae* (26) reveal a monomer in which the dominating secondary feature is an antiparallel β-sheet. The γ-class Cam is remarkably distinct from the α-class carbonic anhydrases in that it is a homotrimer in which each monomer adopts a novel left-handed β-helix fold (28, 36). Even though the α- and γ-classes are notably different in both their tertiary and quaternary structures, both classes contain a catalytically essential zinc ion coordinated by three histidine residues. Recently, the structures of the β-class carbonic anhydrases from both the dicotyledenous plant *Pisum sativum* (pea) (35) and the red alga *Porphyridium purpureum* (41) have been solved. Both the *P. sativum* homo-octamer and the *P. purpureum* homodimer exhibit a predominantly α-helical secondary structure. Unlike enzymes from the α- and γ-classes, the active site zinc of these β-class enzymes is coordinated by two cysteines and one histidine residue. A conserved aspartate residue appears to serve as a fourth ligand in the *P. purpureum* enzyme, but not in the *P. sativum* enzyme.

The kinetic properties of the human α-class isozymes CA I, CA II, and CA III have been extensively investigated and follow a common zinc hydroxide mechanism for catalysis (39, 48). The catalytically active group in this mechanism model is the zinc-bound water, which ionizes to a metal-bound hydroxide ion that attacks CO_2. According to the proposed mechanism, the enzyme-catalyzed reaction occurs in two mechanistically distinct steps (where E = enzyme and B = buffer). The first step is the interconversion between carbon dioxide and bicarbonate (equations 2a and 2b), in which the rate is related to the steady-state parameter k_{cat}/K_m. The second step is the regeneration of the active form of the enzyme (equations 2c

* Corresponding author. Mailing address: Department of Biochemistry and Molecular Biology, The Pennsylvania State University, University Park, PA 16802. Phone: (814) 863-5721. Fax: (814) 862-6217. E-mail: jgf3@psu.edu.

† Present address: Sandvikvagen, S-35241 Vaxjo, Sweden.

and 2d), involving the rate-determining intramolecular and intermolecular proton transfer events which are reflected in the steady-state parameter k_{cat}:

$$E\text{-}Zn^{2+}\text{-}OH^- + CO_2 \rightleftharpoons E\text{-}Zn^{2+}\text{-}HCO_3^- \quad (2a)$$

$$E\text{-}Zn^{2+}\text{-}HCO_3^- + H_2O \rightleftharpoons E\text{-}Zn^{2+}\text{-}H_2O + HCO_3^- \quad (2b)$$

$$E\text{-}Zn^{2+}\text{-}H_2O \rightleftharpoons {}^+H\text{-}E\text{-}Zn^{2+}\text{-}OH^- \quad (2c)$$

$${}^+H\text{-}E\text{-}Zn^{2+}\text{-}OH^- + B \rightleftharpoons E\text{-}Zn^{2+}\text{-}OH^- + BH^+ \quad (2d)$$

The catalytic mechanism of the *M. thermophila* γ-class Cam resembles that of human α-class CA II despite significant structural differences in the active sites of these two enzymes (1). The kinetic properties reported for the *P. sativum* and *Spinacia oleracea* (spinach) β-class carbonic anhydrases are also consistent with this mechanism (29, 30, 46). Thus, the kinetic analyses of enzymes from all three classes suggest convergent evolution of the catalytic mechanism (1, 36, 39).

The β-class was initially thought to be composed solely of carbonic anhydrases from monocotyledenous and dicotyledenous plants. A mitochondrial β-class carbonic anhydrase was discovered in *C. reinhardtii* (18), and other enzymes belonging to this class have since been identified in other algae (25, 62). Only two β-class carbonic anhydrases from the *Bacteria* domain have been purified (22, 53), and the subsequent purification of Cab, a β-class enzyme from the thermophilic archaeon *M. thermoautotrophicum*, establishes that this class of carbonic anhydrase extends to the *Archaea* domain (50). Recent work establishes that this class is widely distributed in metabolically diverse prokaryotes representing both the *Bacteria* and *Archaea* domains and has ancient origins (50, 52).

Even though the β-class of carbonic anhydrase is the only class with documented enzymes in all three domains, less is known about the biochemistry and overall structural aspects of this class than for either the α-class or the more recently identified γ-class. Herein we report on structural and kinetic studies of Cab, the first for any prokaryotic β-class carbonic anhydrase.

MATERIALS AND METHODS

Analytical ultracentrifugation. Equilibrium centrifugation was performed with a Beckman model XLI ultracentrifuge. The radial distribution of protein was monitored by A_{235}, A_{280}, or A_{295}, depending upon the concentration loaded. Protein concentrations of Cab were estimated by using A_{280} and an extinction coefficient (2,740 cm^{-1} M^{-1} based on 1 subunit) calculated from the deduced amino acid sequence of the *cab* gene. Cab was centrifuged at 8,000, 12,000, and 16,000 rpm for 22, 14, and 14 h, respectively. Establishment of equilibrium was verified by the coincidence of the final two scans at each speed. The ultracentrifugation data were fit by using NONLIN (Pharsight Corp., Mountain View, Calif.) and Sedenterp (37).

CD analysis. Spectra were acquired at 37°C with an Aviv circular dichroism (CD) spectrophotometer, model 62DS. The concentration of the *S. oleracea* carbonic anhydrase was estimated by using A_{280} and an extinction coefficient (23,260 cm^{-1} M^{-1} based on 1 subunit) calculated from the deduced amino acid sequence of the *S. oleracea* gene (excluding the 98 N-terminal amino acids encoding the chloroplast transit peptide sequence). Samples (10 μM) of the *M. thermoautotrophicum* Cab and *S. oleracea* carbonic anhydrases in 20 mM potassium phosphate (pH 6.8) containing 0.1 M KCl were placed in a cuvette with a 1-mm path length, and the data points obtained were from 320 to 202 nm in 1.0-nm increments. Five spectra were taken for each sample and averaged. The resulting spectra were normalized for direct comparison.

EXAFS. Zn K-edge X-ray absorption spectroscopy (XAS) data of the as-isolated *M. thermoautotrophicum* ΔH carbonic anhydrase (Cab) were collected on beam line 7-3 at the Stanford Synchrotron Radiation Laboratory, with the SPEAR ring operating at 3.0 GeV and a 50- to 100-mA current (Table 1) (47). For XAS, 180 μl of Cab (50 mg/ml) in 50 mM potassium phosphate (pH 6.8) containing 35% glycerol was transferred to a Lucite cuvette covered with Mylar adhesive tape as an X-ray transparent window material, capped, and frozen in liquid nitrogen. Extended X-ray absorption fine structure (EXAFS) data analysis and curve fitting were performed by using EXAFSPAK (http://ssrl.slac.stanford.edu/exafspak.html) and Feff v7.0 (5, 44). Multiple-scattering contributions from outer-shell atoms of histidine ligands were quantified as described previously (15), with parameters derived from tetra(imidazole) zinc(II) perchlorate (7).

TABLE 1. Collection of X-ray absorption spectroscopic data

Characteristic	Zn EXAFS result
Synchrotron radiation facility	Stanford Synchrotron Radiation Laboratory
Beamline	7-3
Current in storage ring (mA)	50–100
Monochromator crystal	Si[220]
Detection method	Fluorescence
Detector type	Solid-state array[a]
Scan length (min)	25
No. of scans in average	12
Temp (K)	10
Energy standard	Zn foil, first inflection
Energy calibration (eV)	9,660.7
E_0 (eV)	9,670
Pre-edge background (eV):	
Energy range	8,657–9625
Gaussian center	8,638
Width	750
Spline background energy range; eV (polynomial order)	9,333–9,902 (4) 9,902–10,134 (4) 10,134–10,366 (4)

[a] The 13-element Ge solid-state X-ray fluorescence detector at the Stanford Synchrotron Radiation Laboratory is provided by the National Institutes of Health Biotechnology Research Resource.

Enzyme purification. Cab was heterologously produced in *Escherichia coli* as previously described (50). Thawed cell paste (10 g) was suspended in 20 ml of buffer A (50 mM potassium phosphate [pH 6.8]) and passed twice through a chilled French pressure cell at 138 MPa. The cell lysate was centrifuged at 20,000 × *g* for 20 min to remove cell debris and then centrifuged at 100,000 × *g* for 2 h to remove membranes. The supernatant was loaded onto a 50-ml Q Sepharose (Fast Flow) anion-exchange column (Pharmacia) equilibrated with buffer A. After a 100-ml wash, the column was developed with a 400-ml linear gradient from 0 to 0.75 M KCl. The enzyme eluted between 450 and 550 mM KCl, and fractions containing active enzyme were pooled. The fractions containing active enzyme were raised to 1.5 M $(NH_4)_2SO_4$ and run on a 50-ml Phenyl-Sepharose column (Pharmacia) equilibrated with buffer A plus 1.5 M $(NH_4)_2SO_4$. After a 100-ml wash, the column was developed with a 400-ml linear gradient from 1.5 to 0 M $(NH_4)_2SO_4$ with the enzyme eluting at approximately 100 mM $(NH_4)_2SO_4$. The active fractions were pooled, desalted, and loaded onto a Mono Q 10/10 anion-exchange column (Pharmacia) equilibrated with buffer A. After a 30-ml wash, the column was developed with a 100-ml linear gradient from 0 to 1 M KCl. The enzyme eluted between 460 and 520 mM KCl, and fractions containing active enzyme were pooled, desalted, and stored at −20°C. Carbonic anhydrase activity was measured at room temperature by a modification of the electrometric method of Wilbur and Anderson (60). Protein concentrations were determined by the Bradford method with Bio-Rad dye reagent and bovine serum albumin (Sigma) as the standard (12).

Steady-state kinetics. Initial rates of CO_2 hydration and HCO_3^- dehydration were determined by stopped-flow spectroscopy (KinTek, State College, Pa.) at 25°C by the changing pH indicator method (34). Saturated solutions of CO_2 were prepared by bubbling CO_2 into distilled, deionized water (32.9 mM) at 25°C. The CO_2 concentration ranged from 6 to 24 mM, and the HCO_3^- concentration ranged from 5 to 80 mM. The following buffer-pH indicator pairs (and wavelengths) were used: at pH 5.5 to 6.6, MES [2-(*N*-morpolino)ethanesulfonic acid] (pK_a = 6.1)-chlorophenol red (574 nm); at pH 6.8 to 7.2, MOPS [2-(*N*-morpholino)propanesulfonic acid] (pK_a = 7.2)–*p*-nitrophenol (400 nm); at pH 7.4 to 7.8, HEPES [4-(2-hydroxyethyl)-1-piperazineethanesulfonic acid] (pK_a = 7.5)-phenol red (557 nm); at pH 8.0 to 9.0, TAPS [*N*-tris(hydroxymethyl)methyl-3-aminopropanesulfonic acid] (pK_a = 8.4)–*m*-cresol purple (578 nm). The observed initial rates were corrected for the uncatalyzed rate of the reaction, which was at least five times lower than the catalyzed rate. The steady-state parameters k_{cat} and k_{cat}/K_m and their standard errors were then determined by fitting the observed initial rates to the Michaelis-Menten equation.

The buffer dependence was measured at pH 8.5 (TAPS) and 6.5 (MES) by varying the CO_2 concentration from 6 to 24 mM and the buffer concentration from 5 to 50 mM, maintaining the ionic strength at 0.1 M by addition of sodium sulfate. The observed initial rates were fit to the Michaelis-Menten equation. To

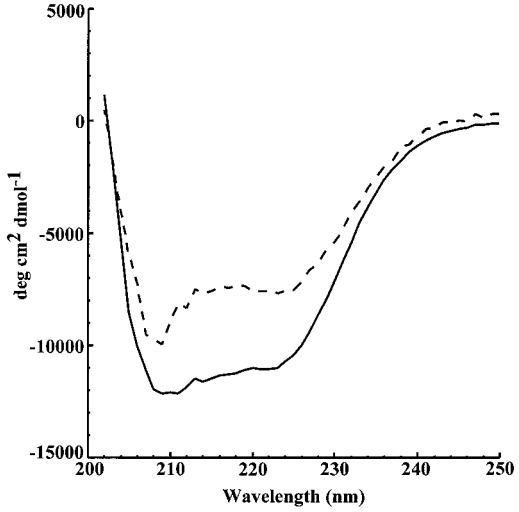

FIG. 1. Comparison of the CD spectra of the *M. thermoautotrophicum* and *S. oleracea* β carbonic anhydrases. Far-UV region spectra of the *S. oleracea* (solid line) and *M. thermoautotrophicum* (dotted line) enzymes are shown.

determine the solvent deuterium isotope effect on the kinetic constants, identical buffer solutions were prepared in H_2O and D_2O. The solvent isotope effect was measured at pH 8.5 (50 mM TAPS). The pH was adjusted until the pH meter readings were identical. This method is appropriate, because the correction of a pH meter reading for pD (pD = meter reading + 0.4) (21) is approximately compensated for by the change in the acid dissociation constant in D_2O for weak acids whose pK_a values lie between 3 and 10 ($pK_D - pK_H = 0.5 \pm 0.1$) (8). The CO_2 concentrations ranged from 7 to 27 mM based on the saturating solutions of CO_2 in D_2O at 25°C (38.1 mM). All fits described were performed with KaleidaGraph (Synergy Software, Reading, Pa.).

RESULTS

Analytical ultracentrifugation analysis. Gel filtration analysis had previously suggested that Cab is a tetramer (50). More precise analytical ultracentrifugation studies were performed to confirm the quaternary structure. A global fit of the data at several speeds and initial concentrations of enzyme could only be satisfactorily modeled as a single species. The molecular mass of 68,080 Da calculated from such a fit is approximately 91% of the tetrameric mass (74,810 Da) calculated from the deduced amino acid sequence. These results establish that Cab is a homotetramer.

CD spectroscopy. CD spectroscopy was performed on both Cab and the β-class *S. oleracea* enzyme to characterize and compare the secondary structures. The spectra overlap throughout the far-UV region (Fig. 1). Cab has two intense negative bands centered at 223 nm ([θ] = −7,700.5) and 209 nm ([θ] = −9,970.0). This result is similar to the spectrum obtained for the *S. oleracea* enzyme (Fig. 1), which has two intense bands centered at 221 nm ([θ] = −11,078) and 209 nm ([θ] = −12,143). These results suggest that the dominant structure for both enzymes is α-helical (31, 32). The CD spectrum of the tetrameric Cab is less intense than that of the octameric *S. oleracea* enzyme, suggesting that the proportion of α-helical structure in the plant enzyme is greater than that of Cab.

XAS. The Zn K-edge X-ray absorption spectrum for Cab shows a shift in absorption edge position to lower energy compared to Cam, the γ-class carbonic anhydrase from *M. thermophila* (1) (Fig. 2A). This shift is indicative of increased electron density at the Zn atom, resulting from an increase in electron-donating ligands such as sulfur. Similarly, the shift of the main peak in the Fourier transform (FT) of β-class Cab (Fig. 2B) to a longer distance, compared with γ-class Cam, is indicative of a larger proportion of sulfur-containing ligands. The decrease in amplitude of the ca. 3- and 4-Å multiple-scattering peaks in the FT indicates that the Zn^{2+} site of β-class Cab contains fewer histidine ligands than γ-class Cam.

The k^3-weighted EXAFS of Cab (Fig. 2C) are best fit by assuming a $Zn\text{-}S_2(N/O)_2$ coordination environment (cf. fits 3 to 6, Table 2). Bond valence sum (BVS) analysis is an empirical method for correlating the sum of the strength of the metal-ligand bonds, as measured by the bond length, to the oxidation state of the metal (40, 57). BVS confirms that the Zn site has a coordination number of 4 (the BVS value should be approximately equal to the oxidation state of the metal, i.e., 2). The EXAFS can be fit assuming one of the O/N ligands results from histidine imidazole coordination (fit 6, Table 2). This fit results in a slight improvement in goodness-of-fit value (cf. fits 4 and 6, Table 2). However, the Debye-Waller factor (σ_{as}^2) for the multiple scattering paths from outer shell atoms indicates that the contribution of this moiety to the overall EXAFS is small. As such, the population of histidine ligands must be disordered to account for the observed σ_{as}^2 values. This disorder could result from a heterogeneity among the Zn sites or from a Zn-histidine coordination geometry in which the imidazole ring is tilted such that the Zn-N-C bond angles differ significantly for the two sides of the imidazole ring. Thus, the EXAFS results indicate the zinc site of Cab is coordinated by two sulfur and two O/N ligands, with the possibility that one of the O/N ligands results from histidine (cf. fit 4, Table 2; Fig. 2D).

Steady-state kinetic measurements. The pH dependencies of both CO_2 hydration and HCO_3^- dehydration catalyzed by Cab were measured by stopped-flow spectroscopy with the changing pH indicator assay. The progress curves for the hydration of CO_2 and dehydration of HCO_3^- were consistent with Michaelis-Menten kinetics. The efficiency (k_{cat}/K_m) for CO_2 hydration (Fig. 3A) was several fold greater than that for HCO_3^- dehydration (Fig. 3B) over the pH range of 6.5 to 7.5, with a 20-fold difference in efficiency at pH 7.0.

Both the steady-state parameters k_{cat} and k_{cat}/K_m for CO_2 hydration were pH dependent over a range from pH 6.2 to 9.0 and show an increase with increasing pH (Fig. 3A). The $CO_2 + H_2O \rightleftharpoons HCO_3^- + H^+$ equilibrium becomes increasingly shifted towards HCO_3^- at increasing pH, requiring the HCO_3^- dehydration reactions to be performed over the pH range from 5.5 to 7.5. CO_2 hydration was not measured below pH 6.2 by this method for the same reasons. The k_{cat}/K_m for HCO_3^- dehydration decreased with increasing pH (Fig. 3B). Neither pH profile could be fitted to a theoretical titration curve with one, two, or three ionizations.

The rate of CO_2 hydration determined at both pH 6.5 and 8.5 was found to be strongly dependent on the concentration of buffer (Fig. 4). The steady-state parameter k_{cat} at both pH values was buffer dependent in a saturable manner. Replots of the k_{cat} values yielded an effective K_m of 4.8 mM for TAPS at pH 8.5 (Fig. 4A) and 12.7 mM for MES at pH 6.5 (Fig. 4B). These values are typical for the apparent K_m of zwitterionic buffers used in this pH range. These results indicate that the buffer behaves kinetically as a second substrate in a ping-pong mechanism, likely accepting a proton from the enzyme during CO_2 hydration. The rate constant k_{cat}/K_m was not dependent on the concentration of buffer (Fig. 4A and B insets).

The solvent hydrogen isotope effects on the steady-state parameters for CO_2 hydration were measured at pH 8.5 and a concentration of TAPS buffer (50 mM) in which intermolecular proton transfer is not rate limiting. The solvent hydrogen isotope effect on k_{cat} was 2.1 ± 0.1, and no significant effect on k_{cat}/K_m (1.2 ± 0.1) was observed.

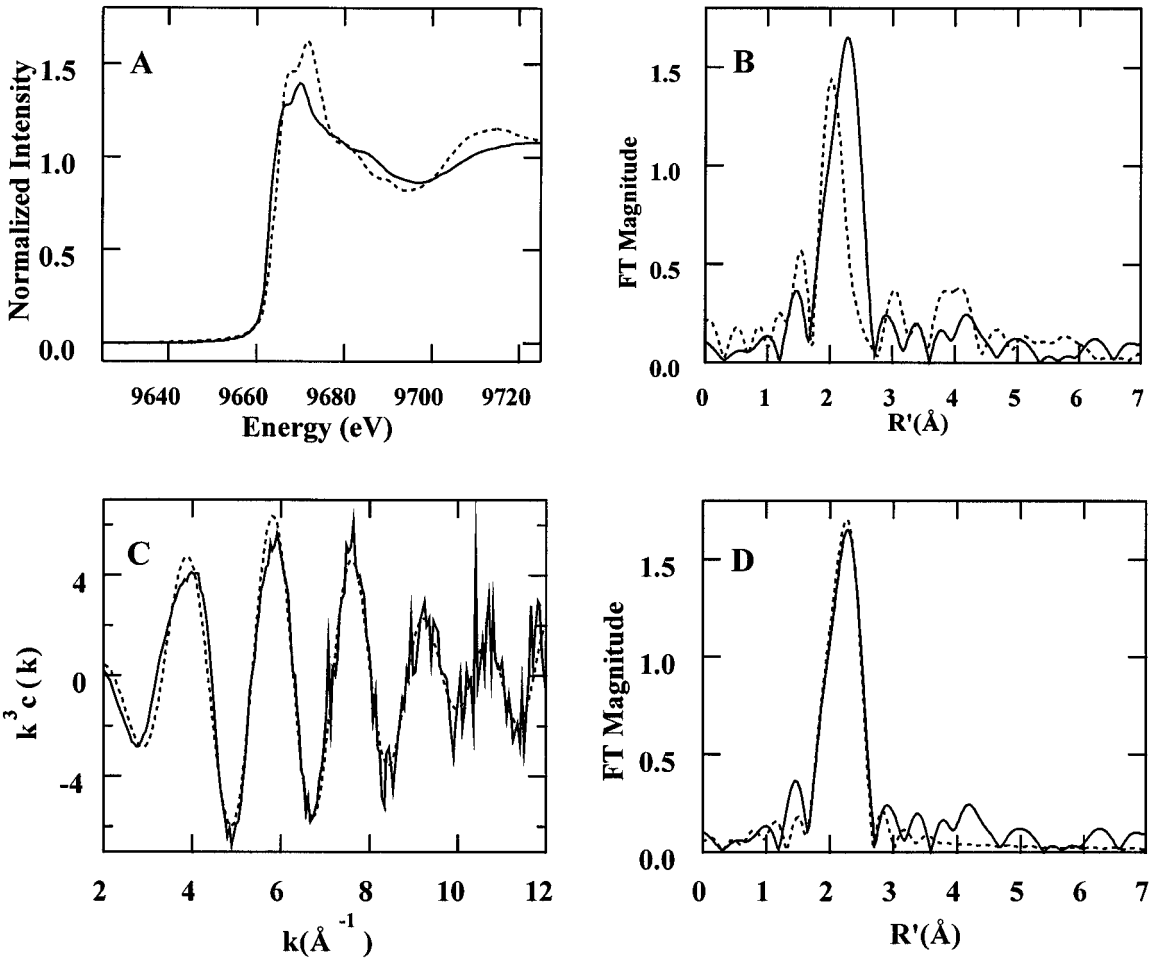

FIG. 2. XAS analysis of Cab. (A and B) X-ray absorption edge spectra (A) and FTs (B) (k = 2 to 12 Å^{-1}) for Cab, the *M. thermoautotrophicum* β-class carbonic anhydrase (solid line), and Cam, the γ-class carbonic anhydrase from *M. thermophila* (dashed line) (1). (C and D) k^3-weighted EXAFS (C) and FTs (D) (k = 2 to 12 Å^{-1}) of the β-class Cab (solid line) and calculated results for $ZnS_2(N/O)_2$ (dashed line; fit 4, Table 2).

DISCUSSION

The overall folds of the monomeric mammalian and prokaryotic *N. gonorrhoeae* α-class carbonic anhydrases are similar, with the antiparallel β-sheet as the dominating secondary structure feature (26). The crystal structure of Cam, the prototypic γ-class carbonic anhydrase, reveals a homotrimer with the monomer adopting a novel left-handed β-helix fold (36). In stark contrast to the mainly β-sheet structures of α- and γ-class carbonic anhydrases, CD analysis of Cab and the *S. oleracea* enzyme suggests a predominantly α-helical structure. These prokaryotic and eukaryotic β-class carbonic anhydrases are from organisms at the phylogenetic extremes, suggesting this secondary structure feature is common to all β-class enzymes; indeed, the crystal structures of the *P. sativum* and *P. purpureum* β-class enzymes reveal a predominance of α-helical structure (35, 41). The content and arrangement of the predicted secondary structure elements for Cab are similar to those of the other β-class carbonic anhydrases (Fig. 5), suggesting a common ancestor, even though the amino acid sequence of Cab is only 23.3% identical to that of the *S. oleracea* enzyme.

Nondenaturing polyacrylamide gel electrophoresis and gel filtration chromatography have previously suggested that the β-class carbonic anhydrases from monocotyledenous plants are homodimeric (43) and those from dicotyledenous plants are homooctameric (9); however, a more precise molecular mass has yet to be reported. In contrast to the enzymes isolated from higher plants, gel filtration studies of Cab and the *E. coli* CynT suggest these prokaryotic enzymes are homotetrameric (22, 50). The more precise analytical ultracentrifugation experiments reported here establish the homotetrameric composition of Cab. Thus, the β-class is distinct from the other two classes in that the β-class carbonic anhydrases are either dimeric, tetrameric, or octameric.

Based on electron microscopy of the chickpea leaf β-class carbonic anhydrase, Aliev et al. (4) presented a model for the quaternary structure of the β-class enzymes from dicotyledenous plants and proposed a 422 (dimer of tetramers) point group symmetry for the eight subunits. Two invariant cysteines (Cys-269 and Cys-272) in the deduced amino acid sequences of β-class carbonic anhydrases from dicotyledenous plants appear necessary for the oligomeric state of the *P. sativum* chloroplast carbonic anhydrase (9). Studies of these invariant cysteines fit well with the electron microscopy studies indicating a double-layered structure in which each layer is a tetramer. However, the recently solved structure of the *P. satvium* enzyme indicates the octamer does not have the predicted 422 point of symme-

TABLE 2. Curve-fitting results for Zn EXAFS[a]

Fit	Shell	N_S	R_{as} (Å)	σ_{as}^2 (Å^2)	ΔE_0 (eV)	f[b]	BVS[c]
1	Zn-O	4	2.10	0.0054	4.38	0.131	1.37
2	Zn-O	3	2.03	0.0031	−1.35	0.072	1.78
	Zn-S	1	2.32	−0.0011			
3	Zn-O	3	2.01	0.0058	−3.65	0.080	2.45
	Zn-S	2	2.30	0.0035			
4	Zn-O	2	2.00	0.0016	−4.86	0.073	2.03
	Zn-S	2	2.30	0.0022			
5	Zn-O	2	1.99	0.0042	−5.91	0.081	2.67
	Zn-S	3	2.29	0.0057			
6	Zn-S	2	2.30	0.0023	−4.42	0.070	2.03
	Zn-O,N	2	2.00	0.0016			
	Zn-C	1	2.99	0.0092			
	Zn-C	1	[3.06]	[0.0092]			
	Zn-C	1	[4.15]	[0.0132]			
	Zn-N	1	[4.19]	[0.0132]			

[a] The sample used was *M. thermoautotrophicum* β-CA. The Stanford Synchrotron Radiation Laboratory file number is ZTC0A (k range = 2 to 12 Å^{-1}). $\Delta k^3\chi = 12.38$. Each group is the chemical unit defined for the multiple scattering calculation. N_S is the number of scatterers (or groups) per metal. R_{as} is the metal-scatterer distance. σ_{as}^2 is a mean square deviation in R_{as}. ΔE_0 is the shift in E_0 for the theoretical scattering functions. Numbers in square brackets were constrained to be either a multiple of the above value (σ_{as}^2) or to maintain a constant difference from the above value (R_{as}).

[b] f is a normalized error (chi squared):

$$f = \frac{\{\sum_i [k^3(\chi_i^{obs} - \chi_i^{calc})]^2/N\}^{1/2}}{[(k^3\chi^{obs})_{max} - (k^3\chi^{obs})_{min}]}$$

[c] $BVS = \Sigma_{exp}[(r_0\text{-}r)/B]$, B = 0.37, $r_0(Zn^{2+}\text{-O}) = 1.704$, and $r_0(Zn^{2+}\text{-S}) = 2.09$.

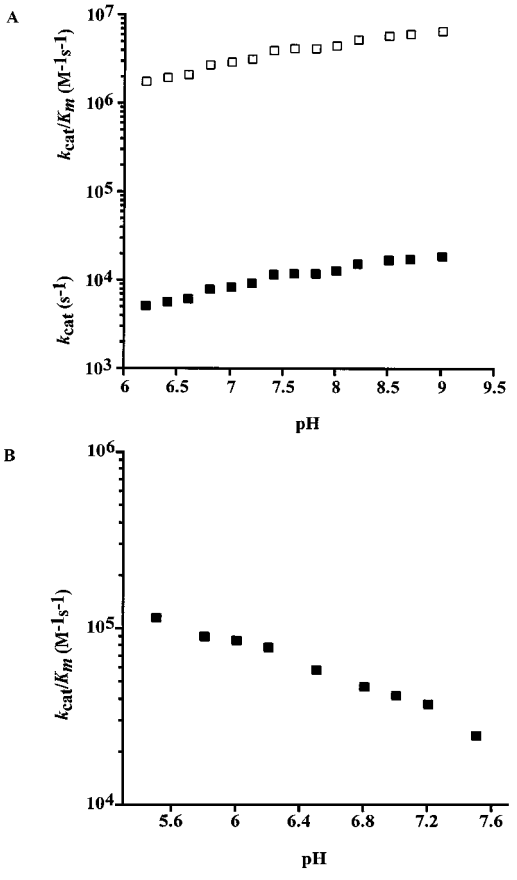

FIG. 3. pH dependence of CO_2 hydration and HCO_3^- dehydration. Activities were measured at 25°C in 50 mM buffer with an ionic strength of 0.1 M. (A) CO_2 hydration. Using Cab concentrations of 1.5 to 1.9 μM, the observed steady-state parameters k_{cat} (■) and k_{cat}/K_m (□) were determined over a pH range of 6.2 to 9.0. (B) HCO_3^- dehydration. Using Cab concentrations of 0.8 to 1.8 μM, the k_{cat}/K_m (■) was determined over a pH range of 5.5 to 7.5.

try, but rather has a 222 (dimer of dimers) symmetry (35). The dimeric *P. purpureum* enzyme, in which each monomer is composed of two internally repeated structures each having an active site (Fig. 5), appears as a tetramer with a pseudo 222 symmetry (41). Why alterations to the invariant Cys-269 and Cys-272 of the dicotyledenous plant enzymes convert the octamer into a tetramer is unclear.

In the *P. sativum* enzyme, pairs of monomers are joined together through extensive interactions mediated by the α1 and α2 helices and β2 strands (35). The dimer is therefore the basic building block, and nearly all of the protein-protein interactions responsible for forming the loosely packed octamer from dimers are mediated through interactions of the β5 strand. However, the second half of the β5 strand, which mediates most of the oligomerization interactions, is absent in several β-class enzymes, including Cab (Fig. 5). How the dimers are held together in the tetrameric Cab awaits solution of its crystal structure.

XAS analysis clearly indicates that the zinc coordination of β-class Cab is distinct from that of the α- and γ-class carbonic anhydrases (cf. fit 4, Table 2; Fig. 2D). The active site zinc of the α- and γ-class enzymes is coordinated by three histidines and at least one water molecule (1, 28, 61). In the catalytic mechanism of carbonic anhydrase, the zinc-bound water ionizes to a metal-bound hydroxide ion that attacks CO_2 (equation 2a). EXAFS results suggest that the active site zinc of β-class Cab is coordinated by two cysteine residues and two oxygen/nitrogen ligands, with the possibility that one of the oxygen/nitrogen ligands derives from histidine (Table 2, fit 4). Our results are nearly identical to EXAFS results previously reported for the *S. oleracea* enzyme (11, 46). Cys-32, His-87, and Cys-90 of Cab are completely conserved in all known β-class carbonic anhydrase sequences (Fig. 5). The recently solved crystal structures of the *P. sativum* and *P. purpureum* β-class carbonic anhydrase confirm that the two conserved cysteines and the conserved histidine are ligands to the active site zinc (35, 41). The second oxygen/nitrogen ligand would be expected to be a water molecule; however, the fourth ligand of the recently solved *P. purpureum* crystal structure is a conserved aspartate corresponding to Asp-34 of Cab. Nonetheless, several pieces of evidence suggest that the conserved aspartate is unlikely to act as an essential fourth ligand to the active site zinc in β-class carbonic anhydrases. First, this aspartate has previously been shown not to be essential for zinc coordination or catalytic activity. Site-directed mutagenesis studies with the *S. oleracea* enzyme (11) indicate that alterations to the two conserved cysteine residues and the conserved histidine residue result in inactive variants lacking zinc; however, the variant in which the conserved aspartate was replaced with asparagine retained the active site zinc. Site-directed mutagenesis of the *S. oleracea* enzyme and Cab indicates that the conserved aspartate is not absolutely required for catalytic activity (41; K. S. Smith, C. J. Ingram-Smith, and J. G. Ferry, unpublished data). Second, the *P. purpureum* carbonic anhydrase was crystallized at pH 6.75, and previous reports indicate that essentially no activity was detected for this enzyme below pH 7.0 (62), sug-

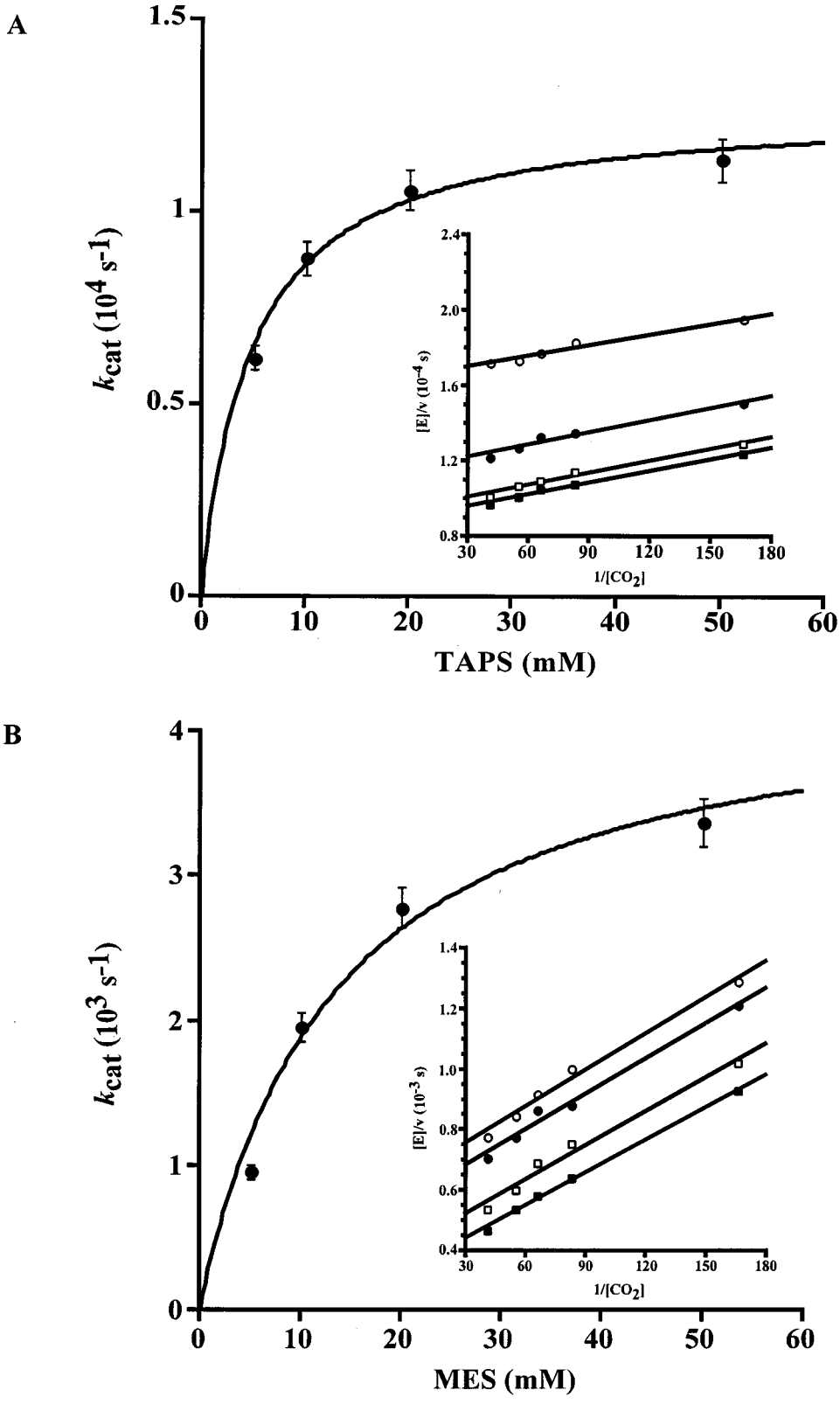

FIG. 4. Buffer dependence of CO_2 hydration. CO_2 hydration was measured at 25°C at pH 8.5 (A) and pH 6.5 (B) with an ionic strength of 0.1 M and a Cab concentration of 2.0 μM. The CO_2 concentration ranged from 6 to 24 mM, and the buffer concentration ranged from 5 to 50 mM. The observed steady-state parameters k_{cat} max and K_m, determined by using the Michaelis-Menten equation, were $(1.3 \pm 0.048) \times 10^4$ s^{-1} and 4.8 ± 0.7 mM, respectively, for TAPS at pH 8.5 and $(4.5 \pm 0.084) \times 10^3$ s^{-1} and 12.7 ± 0.6 mM, respectively, for MES at pH 6.5. (Insets) Double reciprocal plot of observed initial velocities versus CO_2 concentration at different concentrations of TAPS (A) or MES (B) (■, 50 mM; □, 20 mM; ●, 10 mM; ○, 5 mM).

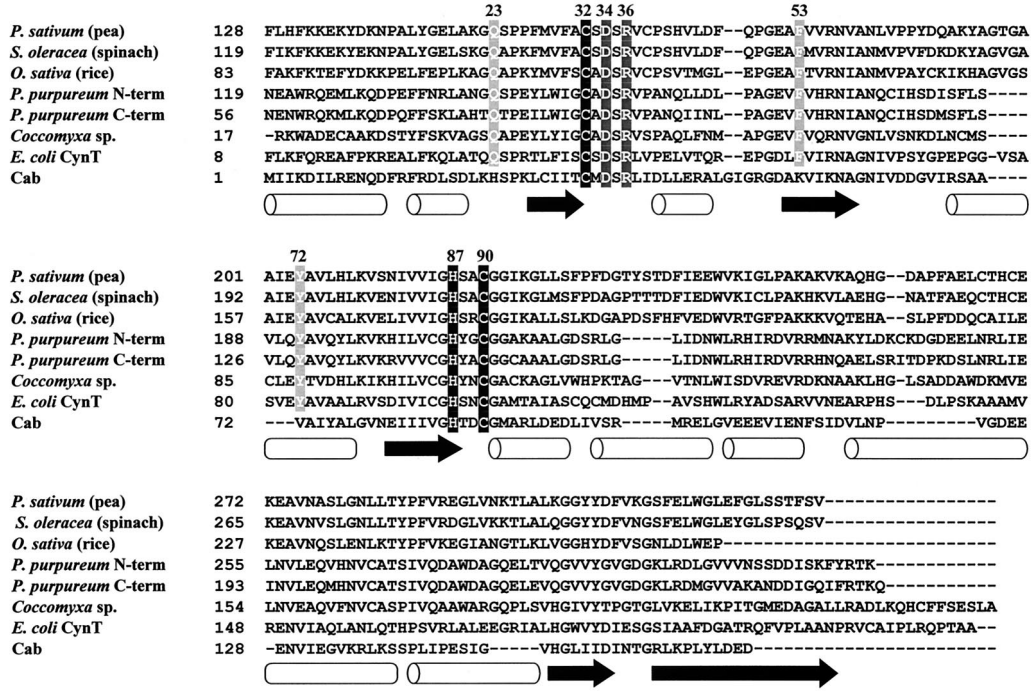

FIG. 5. Alignment of β-class carbonic anhydrase sequences. An alignment of the amino acid sequences of selected β-class carbonic anhydrases was generated with Clustal X (56). The three conserved zinc ligands are shaded in black, and the two other completely conserved amino acids are shaded in dark gray. The three active site residues not conserved in Cab are shaded in light gray. The open barrels indicate α helices as determined from the *P. sativum* structure (35), and the arrows represent β strands. The numbering refers to that of the *M. thermoautotrophicum* Cab amino acid sequence. GenBank accession numbers are as follows: *P. sativum* (pea), 115471; *S. oleracea* (spinach), 115472; *Oryza sativa* (rice), 606817; *P. purpureum*, 1395172; *Coccomyxa* sp., 1663720; *E. coli* CynT, 1657535; and *M. thermoautotrophicum* ΔH Cab, 1272331.

gesting that the published structure of the *P. purpureum* enzyme may be of an inactive enzyme. Therefore, Asp-34 is unlikely to be an essential fourth ligand to the active site zinc in Cab. The second oxygen/nitrogen ligand in Cab is most likely a deprotonated water molecule that serves as the zinc hydroxide attacking CO_2.

Even though the three zinc ligands (Cys-32, His-87, and Cys-90 of Cab) and two other active site residues (Asp-34 and Arg-36 of Cab) are conserved among all β-class carbonic anhydrases (Fig. 5), key active site residues (Gln-151, Phe-179, and Tyr-205 of the *P. sativum* enzyme) conserved among the enzymes from dicotyledenous and monocotyledenous plants, algae, and *E. coli* CynT, are absent in Cab (35). Although the roles of these residues in the *P. sativum* enzyme have not yet been investigated experimentally, Kimber and Pai (35) propose that Gln-151 may electrophilically activate the CO_2 molecule by forming a hydrogen bond with CO_2 through its side chain amide. Phe-179 and Tyr-205 form part of an extensive hydrophobic patch whose function may be to ensure that the binding energy of inhibitor molecules is as unfavorable as possible (35). Other members of the same phylogenetic clade as Cab, which consists primarily of sequences from both archaea and gram-positive bacteria species, are also missing these active site residues present in *P. sativum* (51, 52). In Cab, Gln-151, Phe-179, and Tyr-205 of the *P. sativum* enzyme are substituted for by histidine (His-23), lysine (Lys-53), and valine (Val-72), respectively (Fig. 5). These substitutions imply that the active site of Cab differs substantially from those of other β-class enzymes. Whether His-23, Lys-53, and Val-72 in Cab play a role similar to that proposed for Gln-151, Phe-179, and Tyr-205 in the plant enzymes remains to be investigated.

Although the active sites of the plant β-class carbonic anhydrases and Cab may be significantly different, the kinetic data presented here suggest that the fundamental catalytic mechanism for Cab is similar to that reported for other β-class enzymes. The steady-state parameter k_{cat}/K_m is not dependent on the concentration of buffer, which was shown to act as a second substrate. This result is consistent with the α-class human CA II zinc hydroxide mechanism in which the interconversion of CO_2 and HCO_3^- (equations 2a and 2b), reflected in k_{cat}/K_m, is separate from the intramolecular and intermolecular proton transfer steps (equations 2c and 2d) (14, 34, 48). The pH profile of k_{cat} for the hydration of CO_2 (Fig. 3A) increases with pH, indicating that an unprotonated form of the enzyme is required for catalytic competence, consistent with nucleophilic attack of a zinc-bound hydroxyl group on CO_2. For human CA II, the pH profile of k_{cat}/K_m reveals the pK_a of the zinc-bound water and the pH profile of k_{cat} reveals the pK_a of the proton shuttle residue. The pH profiles of both k_{cat} and k_{cat}/K_m in the direction of CO_2 hydration for Cab (Fig. 3A) show more complicated behavior and could not be fitted to theoretical curves with one, two, or three ionizations. Nearby ionizable groups may influence these pH profiles to produce multiple pK_a values, or the pK_a values are lower than 6.0. The steady-state parameter k_{cat} of the β-class *S. oleracea* carbonic anhydrase was found to be pH dependent, with an apparent pK_a of approximately 8.5 in the absence of sulfate (46). Similar to Cab, the pH profiles for both k_{cat} and k_{cat}/K_m in the direction of CO_2 hydration for the β-class *P. sativum* carbonic anhydrase are pH dependent, although the profiles were not fitted to theoretical titration curves (29).

No significant hydrogen isotope effect was observed on the steady-state parameter k_{cat}/K_m for Cab. This result suggests that D_2O imposes no major structural changes in the enzyme

and that the catalytic steps up to and including the first committed step of the reaction (equations 2a and 2b) do not contain a rate-contributing proton transfer step, consistent with the zinc-hydroxide mechanism. The solvent hydrogen isotope effect on k_{cat} observed for Cab suggests that an intramolecular proton transfer step is at least partially rate determining (equation 2c). Similar isotope effects on k_{cat} were reported for the bovine CA III α-class carbonic anhydrase (45), the γ-class enzyme Cam (1), and the *P. sativum* β-class carbonic anhydrase (30). The observed solvent hydrogen isotope effect on k_{cat} of 2.1 for Cab is smaller than the value of 3.8 reported for human α-class CA II (55), but similar to the value reported for human α-class CA IV (27), which follows a mechanism similar to that of CA II.

M. thermoautotrophicum grows optimally at temperatures between 65 and 75°C, and it is expected that the optimal temperature for enzyme activity would fall in this range; however, the decreased solubility of CO_2 at these temperatures under atmospheric pressure precludes the determination of accurate kinetic parameters above 25°C. In fact, Cab is the most thermostable carbonic anhydrase yet characterized, retaining greater than 90% activity after incubation at 85°C for 15 min (50). Optimal activity aside, the catalytic efficiency (k_{cat}/K_m) for CO_2 hydration (Fig. 3A) was several fold greater than that for HCO_3^- dehydration (Fig. 3B) over the pH range of 6.5 to 7.5, suggesting that the physiological role of Cab is to convert CO_2 to HCO_3^-.

The chemolithoautotrophic *M. thermoautotrophicum* fixes CO_2, and synthesis of oxaloacetate is an important reaction in the CO_2-fixation pathways for the methanoarchaea. Oxaloacetate is the starting point of an incomplete reductive citric acid cycle that terminates at α-ketoglutarate and provides precursors for cell material and coenzyme biosynthesis (49). *M. thermoautotrophicum* possesses two enzymes, pyruvate carboxylase and phosphoenolpyruvate (PEP) carboxylase, for the synthesis of oxaloacetate (49). Bicarbonate has been shown to be the substrate for both of these enzymes; thus, the role of Cab may be to concentrate HCO_3^- in the vicinity of these enzymes. Similarly, eukaryotic carbonic anhydrase has been shown to provide bicarbonate to both pyruvate carboxylase and PEP carboxylase. The α-class human CA V is a mitochondrial enzyme that provides HCO_3^- for pyruvate carboxylase in the liver, kidney, and pancreatic islets (42, 59). In the photosynthesis of C_4 plants, carbonic anhydrase provides bicarbonate to PEP carboxylase for the initial carboxylation reaction in the fixation of CO_2 into C_4 acids (6) by rapidly converting CO_2 entering the mesophyll cells from the atmosphere to HCO_3^-.

Conclusions. Previously, only the plant β-class carbonic anhydrases had been characterized structurally or kinetically. Here we present the first structural and detailed study of a β-class carbonic anhydrase (Cab) from a prokaryote and the first from a chemolithotrophic thermophile. Cab and the enzymes from dicotyledenous plants represent the greatest extremes on the phylogenetic tree of the β-class of carbonic anhydrases (51, 52). The results presented here reveal remarkable similarities between the eukaryotic and prokaryotic enzymes that unite the β-class. Both Cab and the plant enzymes follow a zinc hydroxide mechanism for catalysis. The dominant structure for β-class enzymes is α-helical, and the active site is coordinated by two sulfur and two O/N ligands. These results firmly establish that the α-, β-, and γ-classes are convergently evolved enzymes that, although structurally distinct, are functionally equivalent.

ACKNOWLEDGMENTS

We thank Brandon Doyle for technical assistance with the CD analysis and analytical ultracentrifugation studies and Cheryl Ingram-Smith for assistance with the analytical ultracentrifugation studies. We also thank Matthew Kimber for invaluable discussion of the structure of the *P. sativum* β-class carbonic anhydrase and David Silverman, Cheryl Ingram-Smith, Brian Tripp, and Christie Brosius for critical reading of the manuscript.

This work was supported by grants from the National Institutes of Health to R.A.S. (GM42025) and J.G.F. (GM44661) and NASA-Ames Cooperative Agreement NCC2-1057 to The Pennsylvania State University Astrobiology Research Center (PSARC). The XAS data were collected at the Stanford Synchrotron Radiation Laboratory (SSRL), which is operated by the Department of Energy, Division of Chemical Sciences. The SSRL Biotechnology program is supported by the National Institutes of Health, Biomedical Resource Technology Program, Division of Research Resources. Support for the X-ray fluorescence detector is from NIH BRS Shared Instrumentation grant RR05648.

REFERENCES

1. **Alber, B. E., C. M. Colangelo, J. Dong, C. M. V. Stalhandske, T. T. Baird, C. Tu, C. A. Fierke, D. N. Silverman, R. A. Scott, and J. G. Ferry.** 1999. Kinetic and spectroscopic characterization of the gamma carbonic anhydrase from the methanoarchaeon *Methanosarcina thermophila*. Biochemistry **38:**13119–13128.
2. **Alber, B. E., and J. G. Ferry.** 1994. A carbonic anhydrase from the archaeon *Methanosarcina thermophila*. Proc. Natl. Acad. Sci. USA **91:**6909–6913.
3. **Alber, B. E., and J. G. Ferry.** 1996. Characterization of heterologously produced carbonic anhydrase from *Methanosarcina thermophila*. J. Bacteriol. **178:**3270–3274.
4. **Aliev, D. A., N. M. Guliev, T. G. Mamedov, and V. L. Tsuprun.** 1987. Physiochemical properties and quaternary structure of chick pea carboanhydrase. Biokhimiya **51:**1785–1794.
5. **Andkudinov, A. L., B. Ravel, J. J. Rehr, and S. D. Conradson.** 1998. Real-space multiple scattering calculation and interpretation of x-ray absorption near-edge structure. Physiol. Rev. **58:**7565–7576.
6. **Badger, M. R., and G. D. Price.** 1994. The role of carbonic anhydrase in photosynthesis. Annu. Rev. Plant Physiol. Plant Mol. Biol. **45:**369–392.
7. **Bear, C. A., K. A. Duggen, and H. C. Freeman.** 1975. Tetraimidazolezinc(II) perchlorate. Acta Crystallogr. Sect. B **31:**2713–2715.
8. **Bell, R. P. (ed.)** 1959. The proton in chemistry, p. 183–214. Cornell University Press, Ithaca, N.Y.
9. **Bjorkbacka, H., I. M. Johansson, E. Skarfstad, and C. Forsman.** 1997. The sulfhydryl groups of Cys 269 and Cys 272 are critical for the oligomeric state of chloroplast carbonic anhydrase from *Pisum sativum*. Biochemistry **36:**4287–4294.
10. **Boriack-Sjodin, P. A., R. W. Heck, P. J. Laipis, D. N. Silverman, and D. W. Christianson.** 1995. Structure determination of murine mitochondrial carbonic anhydrase V at 2.45-Å resolution: implications for catalytic proton transfer and inhibitor design. Proc. Natl. Acad. Sci. USA **92:**10949–10953.
11. **Bracey, M. H., J. Christiansen, P. Tovar, S. P. Cramer, and S. G. Bartlett.** 1994. Spinach carbonic anhydrase: investigation of the zinc-binding ligands by site-directed mutagenesis, elemental analysis, and EXAFS. Biochemistry **33:**13126–13131.
12. **Bradford, M. M.** 1976. A rapid and sensitive method for the quantitation of microgram quantities of protein utilizing the principle of protein-dye binding. Anal. Biochem. **72:**248–254.
13. **Chirica, L. C., B. Elleby, B. H. Jonsson, and S. Lindskog.** 1997. The complete sequence, expression in *Escherichia coli*, purification and some properties of carbonic anhydrase from *Neisseria gonorrhoeae*. Eur. J. Biochem. **244:**755–760.
14. **Christianson, D. W., and C. A. Fierke.** 1996. Carbonic anhydrase: evolution of the zinc binding site by nature and by design. Acc. Chem. Res. **29:**331–339.
15. **Cosper, N. J., C. M. V. Stalhandske, H. Iwasaki, T. Oshima, R. A. Scott, and T. Iwasaki.** 1999. Structural conservation of the isolated zinc site in archaeal zinc-containing ferredoxins as revealed by x-ray absorption spectroscopic analysis and its evolutionary implications. J. Biol. Chem. **274:**23160–23168.
16. **Eriksson, A. E., P. M. Kylsten, T. A. Jones, and A. Liljas.** 1988. Crystallographic studies of inhibitor binding sites in human carbonic anhydrase II: a pentacoordinated binding of the SCN^- ion to the zinc at high pH. Proteins Struct. Funct. Genet. **4:**283–293.
17. **Eriksson, A. E., and A. Liljas.** 1993. Refined structure of bovine carbonic anhydrase-III at 2.0 angstrom resolution. Proteins Struct. Funct. Genet. **16:**29–42.
18. **Eriksson, M., J. Karlsson, Z. Ramazanov, P. Gardestrom, and G. Samuelsson.** 1996. Discovery of an algal mitochondrial carbonic anhydrase: molecular cloning and characterization of a low-CO_2-induced polypeptide in *Chlamydomonas reinhardtii*. Proc. Natl. Acad. Sci. USA **93:**12031–12034.
19. **Fukuzawa, H., S. Fujiwara, A. Tachiki, and S. Miyachi.** 1990. Nucleotide

sequences of two genes CAH1 and CAH2 which encode carbonic anhydrase polypeptides in *Chlamydomonas reinhardtii*. Nucleic Acids Res. **18:**6441–6442.

20. **Fukuzawa, H., S. Fujiwara, Y. Yamamoto, M. L. Dionisio-Sese, and S. Miyachi.** 1990. cDNA cloning, sequence, and expression of carbonic anhydrase in *Chlamydomonas reinhardtii*—regulation by environmental CO_2 concentration. Proc. Natl. Acad. Sci. USA **87:**4383–4387.
21. **Glasoe, P. K., and F. A. Long.** 1960. Use of glass electrodes to measure acidities in deuterium oxide. J. Phys. Chem. **64:**188–190.
22. **Guilloton, M. B., J. J. Korte, A. F. Lamblin, J. A. Fuchs, and P. M. Anderson.** 1992. Carbonic anhydrase in *Escherichia coli*. A product of the *cyn* operon. J. Biol. Chem. **267:**3731–3734.
23. **Hakansson, K., and A. Wehnert.** 1992. Structure of cobalt carbonic anhydrase complexed with bicarbonate. J. Mol. Biol. **228:**1212–1218.
24. **Hewett-Emmett, D., and R. E. Tashian.** 1996. Functional diversity, conservation, and convergence in the evolution of the α-, β-, and γ-carbonic anhydrase gene families. Mol. Phylogenet. Evol. **5:**50–77.
25. **Hiltonen, T., J. Karlsson, K. Palmqvist, A. K. Clarke, and G. Samuelsson.** 1995. Purification and characterisation of an intracellular carbonic anhydrase from the unicellular green alga *Coccomyxa*. Planta **195:**345–351.
26. **Huang, S., Y. Xue, E. Sauer-Eriksson, L. Chirica, S. Lindskog, and B. H. Jonsson.** 1998. Crystal structure of carbonic anhydrase from *Neisseria gonorrhoeae* and its complex with the inhibitor acetazolamide. J. Mol. Biol. **283:**301–310.
27. **Hurt, J. D., C. Tu, P. J. Laipis, and D. N. Silverman.** 1997. Catalytic properties of murine carbonic anhydrase IV. J. Biol. Chem. **272:**13512–13518.
28. **Iverson, T. M., B. E. Alber, C. Kisker, J. G. Ferry, and D. C. Rees.** 2000. A closer look at the active site of γ-class carbonic anhydrase: high-resolution crystallographic studies of the carbonic anhydrase from *Methanosarcina thermophila*. Biochemistry **39:**9222–9231.
29. **Johansson, I. M., and C. Forsman.** 1993. Kinetic studies of pea carbonic anhydrase. Eur. J. Biochem. **218:**439–446.
30. **Johansson, I. M., and C. Forsman.** 1994. Solvent hydrogen isotope effects and anion inhibition of CO_2 hydration catalysed by carbonic anhydrase from *Pisum sativum*. Eur. J. Biochem. **224:**901–907.
31. **Johnson, W. C. J.** 1992. Analysis of circular dichroism spectra. Methods Enzymol. **210:**426–447.
32. **Johnson, W. C. J.** 1990. Protein secondary structure and circular dichroism: a practical guide. Proteins **7:**205–214.
33. **Kannan, K. K., B. Notstrand, K. Fridborg, S. Lovgren, A. Ohlsson, and M. Petef.** 1975. Crystal structure of human erythrocyte carbonic anhydrase B. Three-dimensional structure at a nominal 2.2-Å resolution. Proc. Natl. Acad. Sci. USA **72:**51–55.
34. **Khalifah, R. G.** 1971. The carbon hydroxide hydration activity of carbonic anhydrase. I. Stop-flow kinetic studies on the native human isozymes B and C. J. Biol. Chem. **246:**2561–2573.
35. **Kimber, M. S., and E. F. Pai.** 2000. The active site architecture of *Pisum sativum* β-carbonic anhydrase is a mirror image of that of α-carbonic anhydrases. EMBO J. **19:**1407–1418.
36. **Kisker, C., H. Schindelin, B. E. Alber, J. G. Ferry, and D. C. Rees.** 1996. A left-hand beta-helix revealed by the crystal structure of a carbonic anhydrase from the archaeon *Methanosarcina thermophila*. EMBO J. **15:**2323–2330.
37. **Lave, T. M., B. D. Shah, T. M. Ridgeway, and S. L. Pelletier.** 1992. Computer-aided interpretation of analytical sedimentation data for proteins, p. 90–125. *In* S. E. Harding, J. C. Horton, and A. J. Rowe (ed.), Analytical ultracentrifugation in biochemistry and polymer science. Royal Society of Chemistry, London, United Kingdom.
38. **Liljas, A., K. K. Kannan, P. C. Bergsten, I. Waara, K. Fridborg, B. Strandberg, U. Carlbom, L. Jarup, S. Lovgren, and M. Petef.** 1972. Crystal structure of human carbonic anhydrase C. Nat. New Biol. **235:**131–137.
39. **Lindskog, S.** 1997. Structure and mechanism of carbonic anhydrase. Pharmacol. Ther. **74:**1–20.
40. **Liu, W., and H. H. Thorp.** 1993. Bond valence sum analysis of metal-ligand bond lengths in metalloenzymes and model complexes. 2. Refined distances and other enzymes. Inorg. Chem. **32:**4102–4105.
41. **Mitsuhashi, S., T. Mizushima, E. Yamashita, M. Yamamoto, T. Kumasaka, H. Moriyama, T. Ueki, S. Miyachi, and T. Tsukihara.** 2000. X-ray structure of β-carbonic anhydrase from the red alga, *Porphyridium purpureum*, reveals a novel catalytic site for CO_2 hydration. J. Biol. Chem. **275:**5521–5526.
42. **Parkkila, A.-K., A. L. Scarim, S. Parkkila, A. Waheed, J. A. Corbett, and W. S. Sly.** 1998. Expression of carbonic anhydrase V in pancreatic beta cells suggests role for mitochondrial carbonic anhydrase in insulin secretion. J. Biol. Chem. **273:**24620–24623.
43. **Reed, M. L., and D. Graham.** 1981. Carbonic anhydrase in plants: distribution, properties, and possible physiological roles. Prog. Phytochem. **7:**47–94.
44. **Rehr, J. J., J. Mustre de Leon, S. I. Zabinsky, and R. C. Albers.** 1991. Theoretical x-ray absorption fine structure standards. J. Am. Chem. Soc. **113:**5136–5140.
45. **Ren, X., B. H. Jonsson, E. Millqvist, and S. Lindskog.** 1988. A comparison of the kinetic properties of native bovine muscle carbonic anhydrase and an activated derivative with modified thiol groups. Biochim. Biophys. Acta **953:**79–85.
46. **Rowlett, R. S., M. R. Chance, M. D. Wirt, D. E. Sidelinger, J. R. Royal, M. Woodroffe, Y. F. Wang, R. P. Saha, and M. G. Lam.** 1994. Kinetic and structural characterization of spinach carbonic anhydrase. Biochemistry **33:**13967–13976.
47. **Scott, R. A.** 1985. Measurement of metal-ligand distances by EXAFS. Methods Enzymol. **117:**414–458.
48. **Silverman, D. N., and S. Lindskog.** 1988. The catalytic mechanism of carbonic anhydrase: implications of a rate-limiting proteolysis of water. Acc. Chem. Res. **21:**30–36.
49. **Simpson, P. G., and W. B. Whitman.** 1993. Anabolic pathways in methanogens, p. 445–472. *In* J. G. Ferry (ed.), Methanogenesis: ecology, physiology, biochemistry, and genetics. Chapman & Hall, London, United Kingdom.
50. **Smith, K. S., and J. G. Ferry.** 1999. A plant-type (β-class) carbonic anhydrase in the thermophilic methanoarchaeon *Methanobacterium thermoautotrophicum*. J. Bacteriol. **181:**6247–6253.
51. **Smith, K. S., and J. G. Ferry.** 2000. Prokaryotic carbonic anhydrases. FEMS Microbiol. Rev. **24:**335–366.
52. **Smith, K. S., C. Jakubziek, T. S. Whittam, and J. G. Ferry.** 1999. Carbonic anhydrase is an ancient enzyme widespread in prokaryotes. Proc. Natl. Acad. Sci. USA **96:**15184–15189.
53. **So, A. K., and G. S. Espie.** 1998. Cloning, characterization and expression of carbonic anhydrase from the cyanobacterium *Synechocystis* PCC6803. Plant Mol. Biol. **37:**205–215.
54. **Stams, T., S. K. Nair, T. Okuyama, A. Waheed, W. S. Sly, and D. W. Christianson.** 1996. Crystal structure of the secretory form of membrane-associated human carbonic anhydrase IV at 2.8-Å resolution. Proc. Natl. Acad. Sci. USA **93:**13589–13594.
55. **Steiner, H., B. H. Jonsson, and S. Lindskog.** 1975. The catalytic mechanism of carbonic anhydrase. Hydrogen-isotope effects on the kinetic parameters of the human C isoenzyme. Eur. J. Biochem. **59:**253–259.
56. **Thompson, J. D., T. J. Gibson, F. Plewniak, F. Jeanmougin, and D. J. Higgins.** 1997. The Clustal X windows interface: flexible strategies for multiple sequence alignment aided by quality analysis tools. Nucleic Acids Res. **25:**4876–4882.
57. **Thorp, H. H.** 1992. Bond valence sum analysis of metal-ligand bond lengths in metalloenzymes and model complexes. Inorg. Chem. **31:**1585–1588.
58. **Tripp, B. C., and J. G. Ferry.** 2000. A structure-function study of a proton transport pathway in the γ-class carbonic anhydrase from *Methanosarcina thermophila*. Biochemistry **39:**9232–9240.
59. **Vincent, S. H., and D. N. Silverman.** 1982. Carbonic anhydrase activity in mitochondria from rat liver. J. Biol. Chem. **257:**6850–6855.
60. **Wilbur, K. M., and N. G. Anderson.** 1948. Electrometric and colorimetric determination of carbonic anhydrase. J. Biol. Chem. **176:**147–154.
61. **Yachandra, V., L. Powers, and T. G. Spiro.** 1983. X-ray absorption spectra and the coordination number of Zn and Co carbonic anhydrase as a function of pH and inhibitor binding. J. Am. Chem. Soc. **105:**6596–6604.
62. **Yagawa, Y., S. Muto, and S. Miyachi.** 1987. Carbonic anhydrase of a unicellular red alga *Porphyridium cruentum* R-1. I. Purification and properties of the enzyme. Plant Cell. Physiol. **28:**1253–1262.